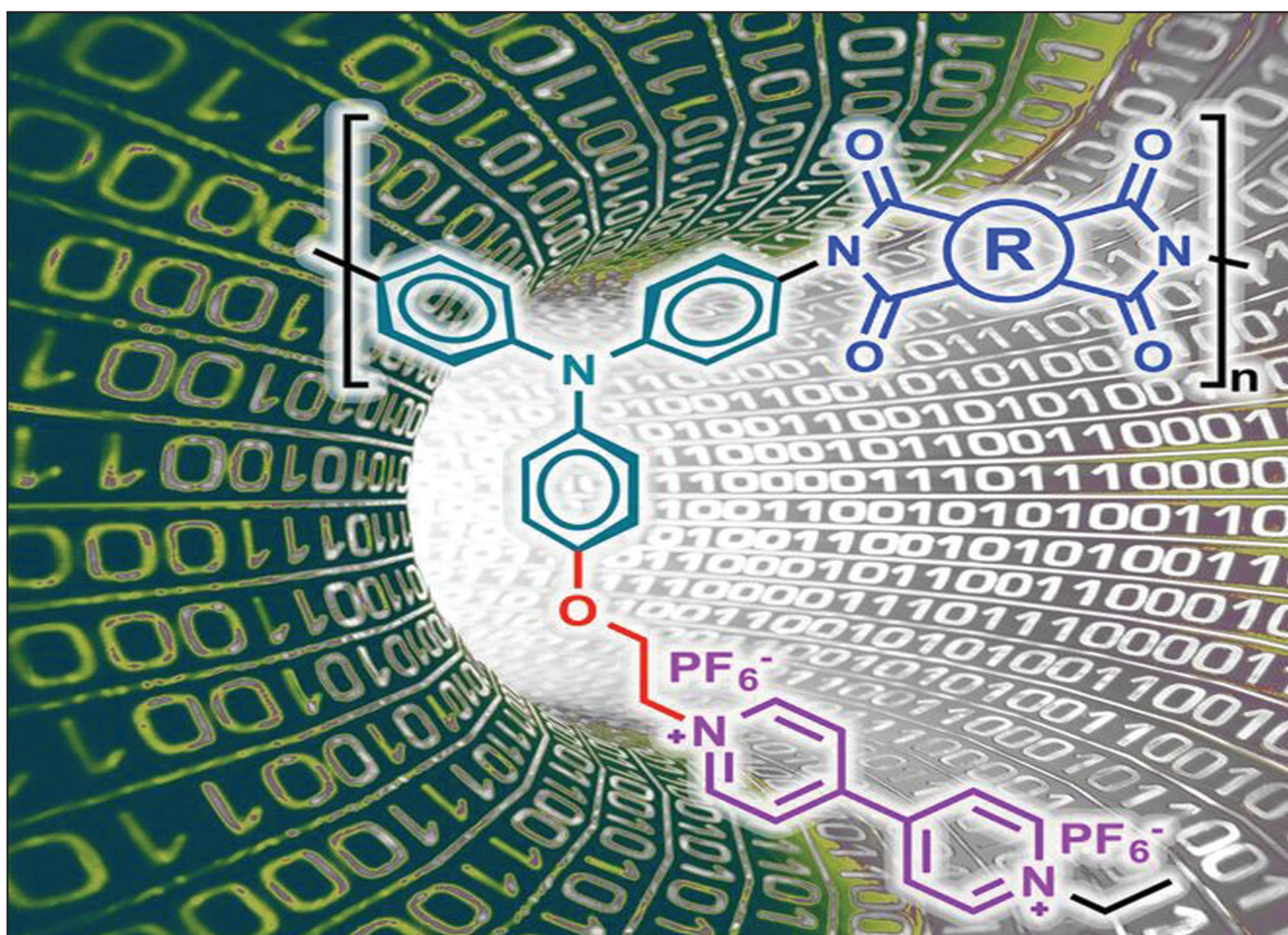




# Macromolecular Rapid Communications



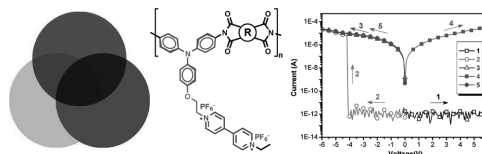
9/2017

WILEY-VCH

# Electrochromism and Nonvolatile Memory Device Derived from Triphenylamine-Based Polyimides with Pendant Viologen Units

Hung-Ju Yen, Chia-Liang Tsai, Shih-Han Chen, Guey-Sheng Liou\*

Three novel solution-processable polyimides containing triphenylamine and pendant viologen moieties are prepared from the newly synthesized diamine and three commercially available dianhydrides. The thermally stable polyimide with strong donor–acceptor charge-transfer possesses write-once read-many-times memory behavior with excellent operation stability. The obtained multicolored electrochromic polymer films reveal ambipolar electrochemical behavior with high optical transmittance contrast of coloration changed from transmissive neutral state to the cyan/magenta/yellow redox states, implying great potential for application in smart window and displays.



## 1. Introduction

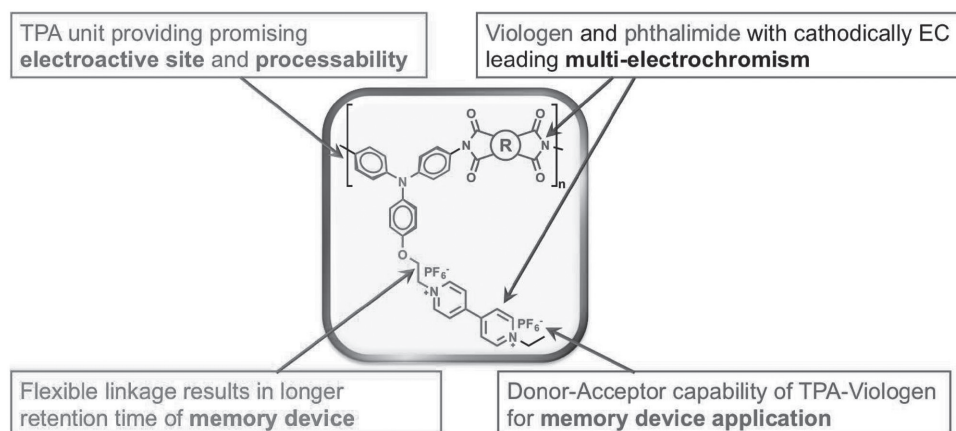
Polymeric materials for optoelectronic device applications have attracted tremendous attention, such as light-emitting diodes,<sup>[1]</sup> photovoltaics,<sup>[2]</sup> electrochromic (EC),<sup>[3]</sup> memory devices,<sup>[3d,4]</sup> and stretchable electronic skin.<sup>[5]</sup> The basic target of a memory device is to demonstrate a method for writing and reading binary digital information of “1” and “0,” which normally arises from changes in intrinsic characteristics/conductivity of materials, such as charge transfer, conformation change, phase change, and redox (reduction–oxidation) reaction, resulted from various electric field or applied voltage, being one of the core functions (primary storage) of modern computers. Different from other memories, a specific device configuration is not necessary for a resistor memory but

the structural design of resistive memory materials is relatively important. Organic small molecules, polymeric, inorganic, and organic/inorganic hybrid materials have been well-established for resistive memories.<sup>[4]</sup> EC materials possess reversible optical changes in transmittance/absorption upon electrochemical redox process, including coordination complexes, conjugated polymers, arylamines, transition metal oxides, and organic molecules.<sup>[6]</sup> Despite that most EC devices at the early development stage are derived from inorganic oxides, organic materials are more advantageous over the former ones owing to their good processability, fast switching ability, high coloration efficiency, and more color changes within a sole material.

Regarding the EC materials, color palettes are significant parameters. The RGB (red–green–blue) and CMY (cyan–magenta–yellow) colors are important since by mixing two of these colors, various colors that are visible can be achieved according to the color merging theory.<sup>[7]</sup> In 2005, our group started the development of high-performance polymers based on arylamines and triphenylamines (TPAs) with interesting coloration and high EC reversibility in the visible region or near-infrared range,<sup>[3c]</sup> even the very first individual transmissive-to-RGB<sup>[8]</sup> and transmissive-to-black<sup>[9]</sup> EC polymers were also successfully prepared. Until now, significant attempts have been continuously invested to design and synthesize new EC

Dr. H.-J. Yen,<sup>[†]</sup> Dr. C.-L. Tsai, S.-H. Chen, Prof. G.-S. Liou  
Functional Polymeric Materials Laboratory  
Institute of Polymer Science and Engineering  
National Taiwan University  
1 Roosevelt Road, 4th Sec., Taipei 10617, Taiwan  
E-mail: gsliau@ntu.edu.tw

<sup>[†]</sup>Present address: Physical Chemistry and Applied Spectroscopy, Chemistry Division, Los Alamos National Laboratory, Los Alamos, NM 87545, USA



■ Figure 1. Structural design strategy of TPA-based polyimides Vio-PI.

polymers with tunable and more saturated coloration. Even though extensive research on the colors of EC polymers have been performed, the construction of transmissive-to-CMY EC polymers remains a crucial issue due to the difficulty and complexity of structural design.

As per the literature, polyimide<sup>[10]</sup> usually exhibits reversible electrochemical reduction reaction with strong coloration changes in the visible spectrum.<sup>[11]</sup> The electroactive site has been recognized as the aromatic-carbonyl within the phthalimide unit. In addition, viologen with a strong electron-withdrawing characteristic also exhibits EC behavior resulting from charge transfer between the colorless viologen dications ( $V^{2+}$ ) and the colored viologen cation radical ( $V^{\cdot+}$ ),<sup>[12]</sup> producing a high optical contrast in the visible range as the reduction–oxidation reaction happens.<sup>[13]</sup> Moreover, the EC color of viologen derivatives can also be fine-tuned with various chain length or structure as substituted groups.<sup>[14]</sup>

Accordingly, in this work we were trying to synthesize novel electroactive TPA-based high-performance polymers with the incorporation of cathodically EC phthalimide and viologen groups for both multicolored EC and polymeric memory applications (Figure 1). By judicious combination of the electron donating/accepting ability and electrochromism derived from TPA, viologen, and phthalimide moieties, the resulting polyimides (PIs) are anticipated to exhibit a stable charge transfer complex and multi-electrochromism. The nonplanar structure of flexible ethyl-linkage might block the back charge transfer and result in an extended retention time of the prepared memory device after removing the applied potential. In addition, the obtained polymers will exhibit high organosolubility due to the incorporation of packing-disruptive propeller-shaped TPA groups into the polymer main chain, which is essential for the large-area fabrication of EC and memory devices via solution casting or spin-coating techniques.

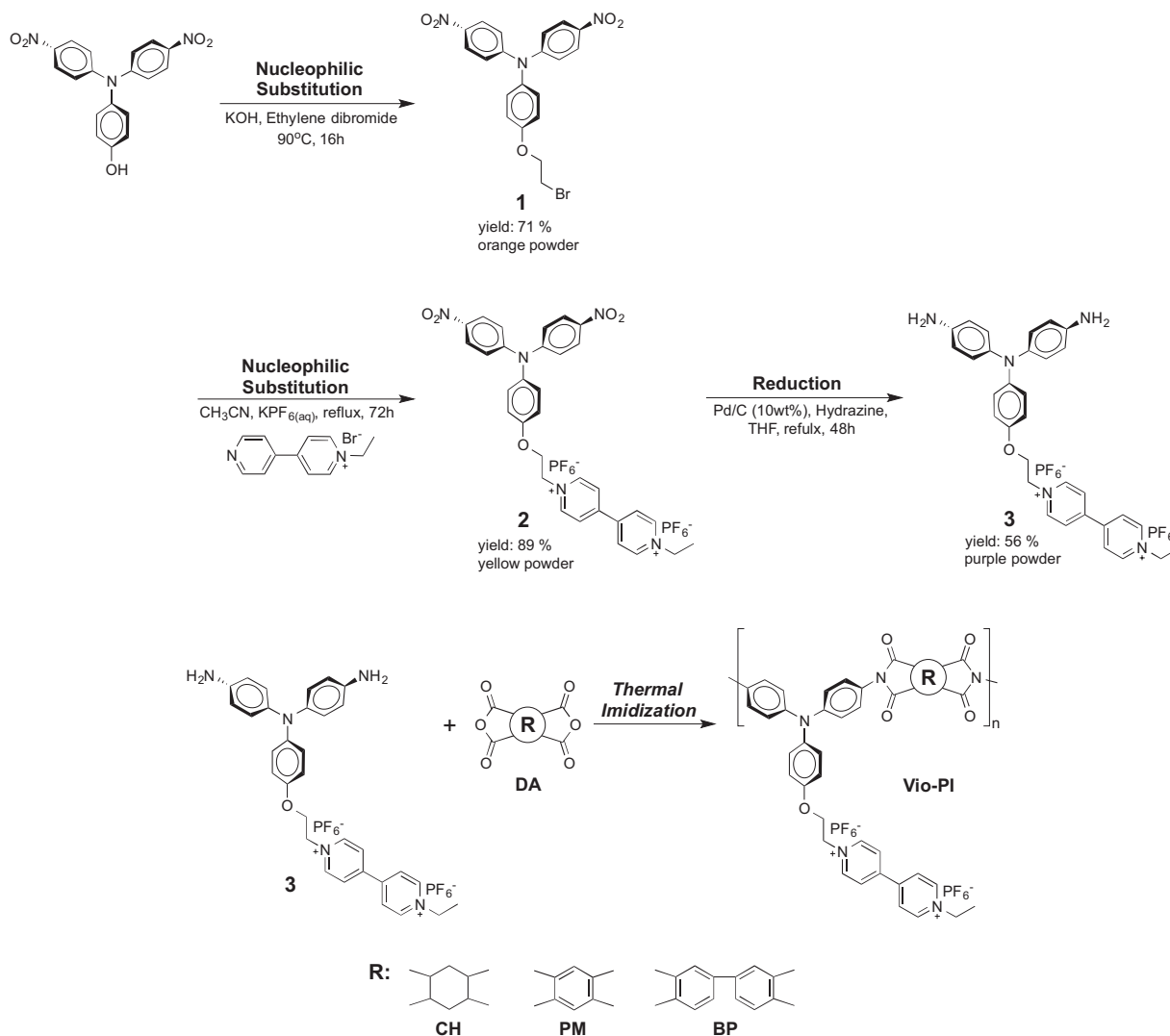
## 2. Results and Discussion

### 2.1. Monomer Synthesis

A TPA-based and viologen-containing diamine monomer, 1-(2-(4-(bis(4-aminophenyl)amino)phenoxy)ethyl)-1'-ethyl-[4,4'-bipyridine]hexafluorophosphate (**3**), was synthesized by palladium-catalyzed reduction of its corresponding dinitro compound, 1-(2-(4-(bis(4-nitrophenyl)amino)phenoxy)ethyl)-1'-ethyl-[4,4'-bipyridine]hexafluorophosphate (**2**), derived from aromatic nucleophilic substitution of 4,4'-dinitro-4''-(2-bromoethoxy)triphenylamine (**1**) with 1-ethyl-4-(4-pyridinyl)pyridinium bromide (Scheme 1). Elemental analysis, NMR, and Fourier transform infrared (FT-IR) spectroscopy are utilized to characterize the structural information of dinitro compounds and the diamine monomer. Figure S1 (Supporting Information) illustrates the FT-IR spectra of the prepared compounds; dinitro-compound **2** possessed two absorption bands at around 1585 and 1307  $\text{cm}^{-1}$  for  $\text{NO}_2$  asymmetric and symmetric stretching, respectively. After the reduction reaction, the typical absorption pair of primary amino group in diamine monomer **3** appeared at 3385 and 3461  $\text{cm}^{-1}$  (N–H stretching) with the disappearance of the absorption bands for nitro group. Figures S2–S8 (Supporting Information) summarized the NMR spectra of the new compounds as well as the assigned carbon and proton, which is interpreted by 2D NMR spectra. Thus, the spectroscopic results and elemental analysis ensure the successful preparation of the TPA-based diamine monomer with pendant viologen group in this work.

### 2.2. Polymer Synthesis

Three PIs, **Vio-CH**, **Vio-PM**, and **Vio-BP**, were synthesized by polycondensation of diamine **3** with commercial



■ Scheme 1. Synthetic route to diamine compound **3** and polyimides **Vio-PI**.

dianhydrides **CHDA**, **PMDA**, and **BPDA**, via thermal imidization, respectively (Scheme 1). The reaction mixtures became viscous during the polymerization and the poly(amic acid)s were further dehydrated to the corresponding PIs under subsequent heating process. The molecular weights and inherent viscosities of **Vio-PI** are listed in Table S1 (Supporting Information). IR spectra of **Vio-PI** in Figure S9 (Supporting Information) exhibit representative imide bands at 1775 (symmetrical C=O), 1720 (symmetrical C=O), and 730  $\text{cm}^{-1}$  (imide ring deformation). Figure S10 (Supporting Information) shows a typical set of  $^1\text{H}$  spectrum of PI **Vio-PM** with the assigned peaks for hydrogen of the recurring unit, and the absence of resonance peak at around 10 ppm further supports the complete thermal imidization.

## 2.3. Polymer Properties

### 2.3.1. Basic Characterization

Solubility of **Vio-PI** has been qualitatively measured and summarized in Table S2 (Supporting Information). **Vio-PI** with high solubility reveals great potential for practical applications by large-area solvent-casting fabrication. Thermal behaviors of **Vio-PI** were also investigated by thermal gravimetric analysis (TGA) and thermomechanical analysis (TMA), and the typical TGA diagrams shown in Figure S11 (Supporting Information) revealed good thermal property with the carbonized residue (char yield) over 54% at 800  $^{\circ}\text{C}$  under nitrogen atmosphere (as summarized in Table S3 in the Supporting Information). Notably, the high char yields of these PIs in air flow could be attributed to the pendant bipyridine salt moiety, which is evidenced by

the TGA curve of model compound **2**, showing a comparable result as PIs. The softening temperature ( $T_s$ ) can be readily obtained by TMA thermograms (as shown in Figure S12 in the Supporting Information).

### 2.3.2. Absorption and Electrochemical Studies

Ultraviolet–visible (UV–vis) spectroscopic results of PI **Vio-CH** is depicted in Figure S13a (Supporting Information) and the energy gap ( $E_g$ ) of the prepared polymers was calculated by the onset wavelength.<sup>[6]</sup> The electrochemistry was tested by cyclic voltammetry (CV) in nitrogen atmosphere, using the PI-coated ITO glass as working electrodes and 0.1 M tetrabutylammonium perchlorate (TBAP) as electrolyte. In addition, anhydrous acetonitrile ( $\text{CH}_3\text{CN}$ ) and propylene carbonate (PC) were employed for oxidation and reduction cycles, respectively. The CV diagrams are shown in Figures S13b and S14 (Supporting Information). **Vio-PM** and **Vio-BP** both revealed one reversible oxidation couple and four reversible reduction redox originating from the TPA, viologen, and dianhydride moieties. In order to manifest the reduction steps in detail, differential pulse voltammograms were investigated and demonstrated four distinct reduction states. Table S4 (Supporting Information) summarized the redox potentials of the PIs with their highest occupied molecular orbital and lowest unoccupied molecular orbital. Moreover, **OMe-PM** and **OMe-BP** structurally related to **Vio-PM** and **Vio-BP** but without viologen pendant groups, were also used to differentiate the electrochemical reduction stages, respectively. From the comparison of reduction processes shown in Figure S14 (Supporting Information), the proposed mechanism of redox reactions summarized in Scheme S1 (Supporting Information) represents a possible electron distribution for the reduced forms and can be described by other resonance forms accompanied with the charge delocalization.

### 2.3.3. Memory Device Characteristics

The memory properties of **Vio-CH** were characterized by the current–voltage ( $I$ – $V$ ) diagrams of a sandwiched ITO-coated PEN/**Vio-CH**/Al device (as shown in Figure 2). The PI film serving as an active layer was spin-coated between ITO and Al. A standard thickness of  $\approx 50$  nm was employed to exclude the thickness effect (Figure 2A).

Figure 2B summarizes the  $I$ – $V$  result of **Vio-CH** memory device. With the first positive and negative scan from 0 to +6/–6 V, the device was initially in the OFF (low conductive) state with a current around  $\approx 10^{-12}$  A, then increased sharply from OFF state to  $\approx 10^{-5}$  A (ON state) at threshold voltages of –4.2 V, showing the transition from OFF to ON state, which is defined as a “writing” process. After the succeeding negative scan (third sweep) and then positive

scan (fourth sweep), the device remained on the ON state, indicating a reading process. The memory device reveals the nonerasable behavior, even apply a reverse electric field or remove the power for a longer period of time (more than a few hours; the fifth sweep). The results reveal that **Vio-CH** film exhibits nonvolatile WORM (write-once read-many-times) memory behavior. Furthermore, the long-term operation at the respective ON and OFF states of the **Vio-CH** memory device with a continuously applied voltage of –1 V was tested and shown in Figure 2C. There is negligible degradation in current at both ON and OFF states after  $10^4$  s under the readout test, indicating an excellent stability of the memory device.

To ensure the reliability of the flexible memory device, we further tested the device with physically fixing by a vernier caliper (Figure 2D). The bending radius of curvature as 11, 9, 7, and 5 mm was applied for the switching performance measurement. This flexible memory device does not crack/deform under severe mechanical bending stress, showing a high feasibility and reproducibility of the memory behavior (Figure 2E).

### 2.3.4. Spectro-Electrochemistry and Electrochromic Properties

The EC behavior was manifested by spectro-electrochemical techniques. Before measurement, PI film was casting on an ITO-coated substrate, and the electrochemical cell was fabricated from a quartz cuvette and placed in a UV–vis near-infrared (NIR) spectrophotometer to collect absorption spectra at various applied potentials. Figure 3 presents the typical spectro-electrochemical spectra of PI films with correlated applied potentials.

Both polymer films reveal a strong absorption in the UV–vis region (301 nm for **Vio-PM**, 328 nm **Vio-BP**) as the  $\pi$ – $\pi^*$  transition in the TPA moieties. After oxidation by raising the applied potential from 0.00 to 1.05 V, both polymer films undergo similar changes, where the intensity of neutral absorptions gradually diminished and two new peaks at 370/740 nm and 382/742 nm for **Vio-PM** and **Vio-BP** gradually increased in intensity, respectively, which can be attributed to the production of a monocation radical of the nitrogen in TPA unit.<sup>[3c,d]</sup> From the inset shown in Figure 3A,C, the color of PI films changed from the transmissive colorless neutral state (pale yellow; 0.00 V) to the highly coloring oxidation state (dark cyan; 1.05 V) with a high optical transmittance change ( $\Delta T\%$ ) of 64% and 50% for **Vio-PM** and **Vio-BP**, respectively.

Figure 3B exhibits new absorption peaks at 561 and 725 nm, gradually increasing in the reduction process to the high  $\Delta T\%$  of 47% and 40%, respectively. Accordingly, the color of **Vio-PM** thin film changes from a transmissive colorless neutral state (pale yellow; 0.00 V) through

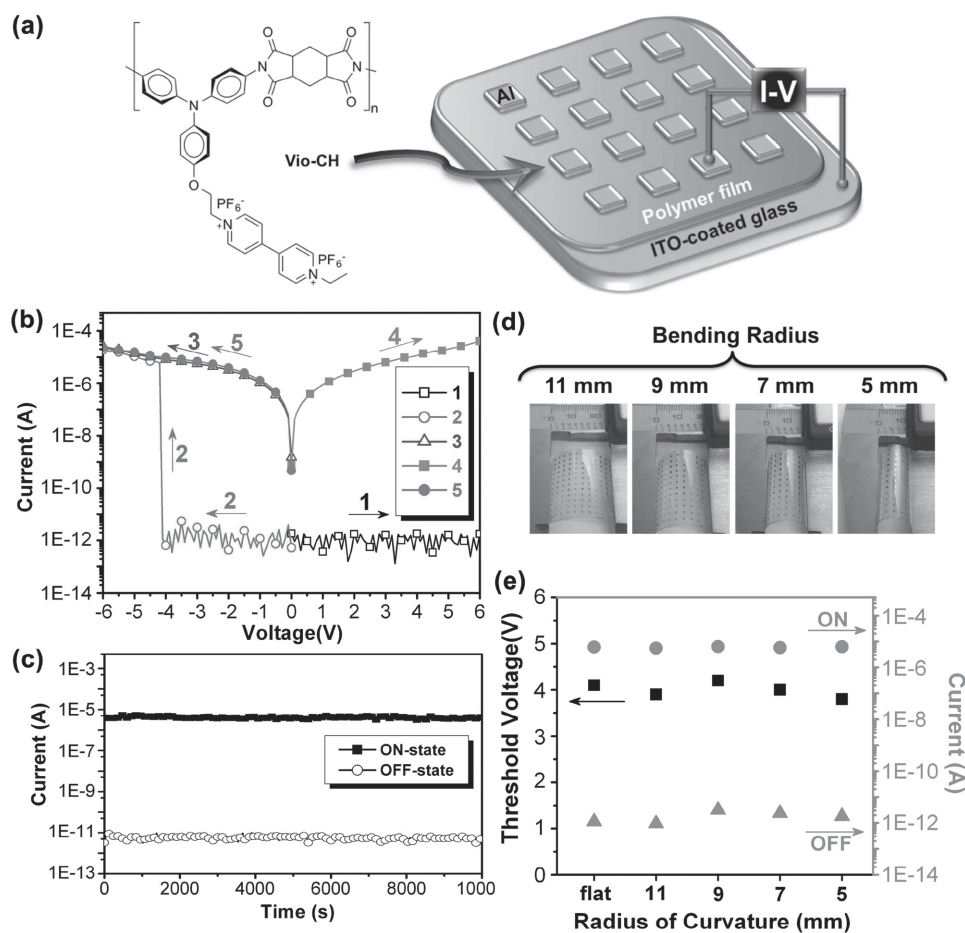


**Figure 2.** A) Chemical structures of **Vio-CH** and the memory device configuration. B)  $I$ - $V$  curves of **Vio-CH** memory device (the fifth sweep is operated after removing the power for 3 h). C) Retention times on the ON and OFF states with a continuously applied voltage of  $-1$  V. D) Illustration of flexible memory device in different bent states. E) Variation of threshold voltage and current with different bending radius of the **Vio-CH** flexible memory device.

the first (light purple;  $-0.55$  V), second (dark purple;  $-0.85$  V), third (light green;  $-1.35$  V) to the fully reduced state (magenta;  $-1.75$  V), respectively. Interestingly, upon reduction of **Vio-BP** PI film to the first reduced state (from 0.00 to  $-0.55$  V), new peaks at 609 and 874 nm gradually increased in intensity but decreased rapidly after further reduction to  $-0.95$  V, corresponding to the second reduced state (Figure 3D). When the reduction potential was even high to  $-1.50$  V, the new peaks at 626 and 866 nm continuously increased with high  $\Delta T\%$  of 66% and 60%, respectively. The inset in Figure 3D depicts the color of **Vio-BP** PI film switching from a transmissive neutral state (pale yellow; 0.00 V) through the first (purple;  $-0.55$  V), second (dark yellow;  $-0.95$  V), third (dark olive green;  $-1.35$  V) to the fully reduced state (navy;  $-1.75$  V), respectively. In addition, the coloration is well-distributed across the polymer films with high  $\Delta T\%$ . Thus, by summarizing the EC results, the novel PIs based on TPA and pendant viologen moieties demonstrate a great combination

of redox units for the preparation of CMY primary-EC materials.

### 3. Conclusions

Three novel solution-processable polyimides containing TPA and pendant viologen moieties were prepared from the diamine, 1-(2-(4-(bis(4-aminophenyl)amino)phenoxy)ethyl)-1'-ethyl-[4,4'-bipyridine]hexafluorophosphate (**3**), and three commercially available dianhydrides. The thermally stable polyimide with strong donor-acceptor charge-transfer possesses WORM memory behavior with excellent operation stability. The obtained multicolored EC polymer films revealed ambipolar electrochemical behavior with high optical transmittance contrast of coloration changed from transmissive neutral state to the cyan/magenta/yellow redox states. The results suggest a great potential of these new high-performance

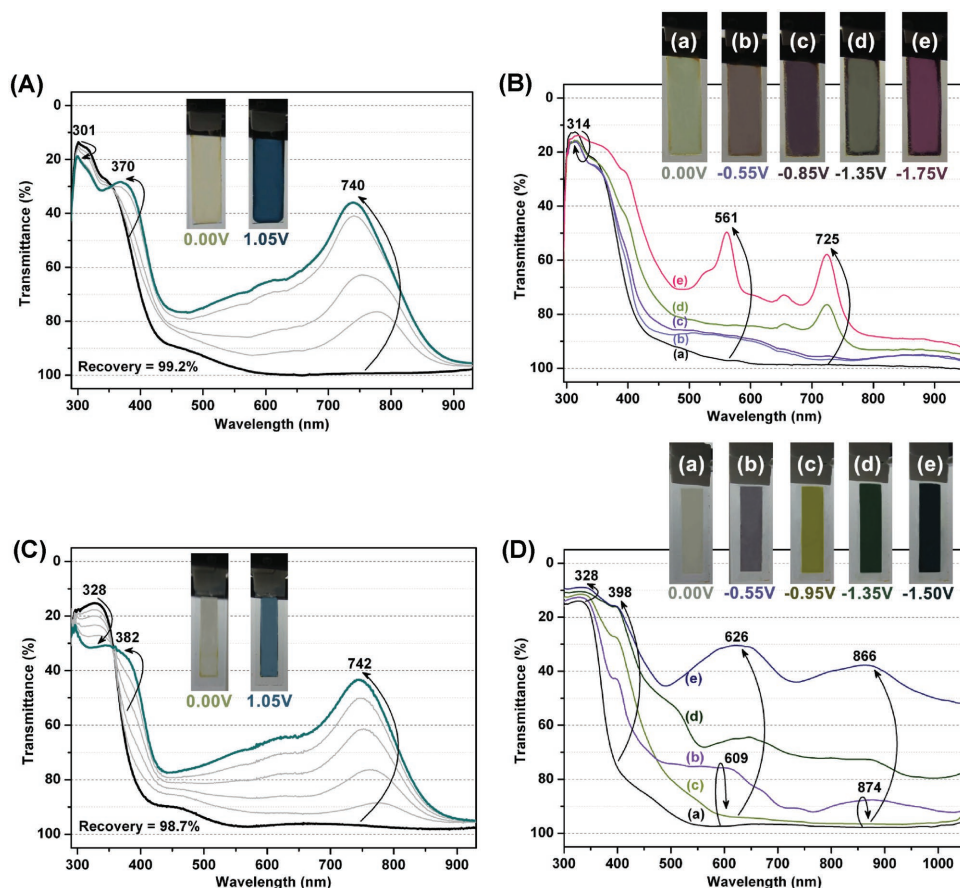


**Figure 3.** Electrochromic behavior of PIs **Vio-PM** and **Vio-BP** thin films ( $\approx 115$  nm in thickness) in 0.1 M TBAP/CH<sub>3</sub>CN or PC. Applied potential for **Vio-PM**: A) 0.00 to 1.02, B) (a) 0.00, (b)  $-0.55$ , (c)  $-0.85$ , (d)  $-1.35$ , and (e)  $-1.75$  (V vs Ag/AgCl). Applied potentials for **Vio-BP**: C) 0.00 to 1.05, D) (a) 0.00, (b)  $-0.55$ , (c)  $-0.95$ , (d)  $-1.35$ , and (e)  $-1.50$  (V vs Ag/AgCl).

polyimides with multifunctionality for flexible electronics applications.

## Supporting Information

Supporting Information is available from the Wiley Online Library or from the author.

Acknowledgements: H.-J.Y. and C.-L.T. contributed equally to this work. The authors would like to acknowledge financial support by the Ministry of Science and Technology of Taiwan.

Received: November 18, 2016; Revised: January 22, 2017;  
Published online: March 2, 2017; DOI: 10.1002/marc.201600715

Keywords: electrochromism; memory device; polyimide; triphenylamine; viologen

[1] a) C.-Y. Lu, M. Jiao, W.-K. Lee, C.-Y. Chen, W.-L. Tsai, C.-Y. Lin, C.-C. Wu, *Adv. Funct. Mater.* **2016**, *26*, 3250; b) S. Y. Lee, T. Yasuda, H. Komiyama, J. Lee, C. Adachi, *Adv. Mater.* **2016**,

*28*, 4019; c) D. J. Harkin, K. Broch, M. Schreck, H. Ceymann, A. Stoy, C.-K. Yong, M. Nikolka, I. McCulloch, N. Stingelin, C. Lambert, H. Sirringhaus, *Adv. Mater.* **2016**, *28*, 6378.

[2] a) S. Shi, J. Yuan, G. Ding, M. Ford, K. Lu, G. Shi, J. Sun, X. Ling, Y. Li, W. Ma, *Adv. Funct. Mater.* **2016**, *26*, 5669; b) W. J. Dong, J. Y. Park, J. Ham, G. H. Jung, I. Lee, J.-L. Lee, *Adv. Funct. Mater.* **2016**, *26*, 5437; c) S.-J. Ko, B. Walker, T. L. Nguyen, H. Choi, J. Seifter, M. A. Uddin, T. Kim, S. Kim, J. Heo, G.-H. Kim, S. Cho, A. J. Heeger, H. Y. Woo, J. Y. Kim, *Adv. Funct. Mater.* **2016**, *26*, 3324.

[3] a) P. M. Beaujuge, J. R. Reynolds, *Chem. Rev.* **2010**, *110*, 268; b) P. M. Beaujuge, C. M. Amb, J. R. Reynolds, *Acc. Chem. Res.* **2010**, *43*, 1396; c) H. J. Yen, G. S. Liou, *Polym. Chem.* **2012**, *3*, 255; d) H.-J. Yen, C.-J. Chen, G.-S. Liou, *Adv. Funct. Mater.* **2013**, *23*, 5307; e) J. Jensen, M. Hösel, A. L. Dyer, F. C. Krebs, *Adv. Funct. Mater.* **2015**, *25*, 2073; f) K. Lin, S. Chen, B. Lu, J. Xu, *Sci. China: Chem.* **2017**, *60*, 38; g) Z. Tong, Y. Tian, H. Zhang, X. Li, J. Ji, H. Qu, N. Li, J. Zhao, Y. Li, *Sci. China: Chem.* **2017**, *60*, 13.

[4] a) Q.-D. Ling, D.-J. Liaw, C. Zhu, D. S.-H. Chan, E.-T. Kang, K.-G. Neoh, *Prog. Polym. Sci.* **2008**, *33*, 917; b) H.-J. Yen, G.-S. Liou, *Polym. J.* **2016**, *48*, 117; c) H.-J. Yen, C. Shan, L. Wang, P. Xu, M. Zhou, H.-L. Wang, *Polymers* **2017**, *9*, 25.

[5] a) K. Hu, R. Xiong, H. Guo, R. Ma, S. Zhang, Z. L. Wang, V. V. Tsukruk, *Adv. Mater.* **2016**, *28*, 3414; b) W. Liu, Z. Chen, G. Zhou, Y. Sun, H. R. Lee, C. Liu, H. Yao, Z. Bao, Y. Cui, *Adv.*

- Mater.* **2016**, *28*, 3578; c) X. Xue, Y. Fu, Q. Wang, L. Xing, Y. Zhang, *Adv. Funct. Mater.* **2016**, *26*, 3128.
- [6] a) R. J. Mortimer, *Chem. Soc. Rev.* **1997**, *26*, 147; b) P. Monk, R. Mortimer, D. Rosseinsky, *Electrochromism and Electrochromic Devices*, Cambridge University Press, New York, **2007**; c) B.-B. Cui, Y.-W. Zhong, J. Yao, *J. Am. Chem. Soc.* **2015**, *137*, 4058; d) C. Fan, C. Ye, X. Wang, Z. Chen, Y. Zhou, Z. Liang, X. Tao, *Macromolecules* **2015**, *48*, 6465; e) C. Reus, M. Stolar, J. Vanderkley, J. Nebauer, T. Baumgartner, *J. Am. Chem. Soc.* **2015**, *137*, 11710; f) K. Takada, R. Sakamoto, S.-T. Yi, S. Katagiri, T. Kambe, H. Nishihara, *J. Am. Chem. Soc.* **2015**, *137*, 4681.
- [7] A. L. Dyer, E. J. Thompson, J. R. Reynolds, *ACS Appl. Mater. Interfaces* **2011**, *3*, 1787.
- [8] L. T. Huang, H. J. Yen, C. W. Chang, G. S. Liou, *J. Polym. Sci., Part A* **2010**, *48*, 4747.
- [9] H. J. Yen, K. Y. Lin, G. S. Liou, *J. Mater. Chem.* **2011**, *21*, 6230.
- [10] I. Willner, A. Riklin, N. Lapidot, *J. Am. Chem. Soc.* **1990**, *112*, 6438.
- [11] a) S. Mazur, P. S. Lugg, C. Yarnitzky, *J. Electrochem. Soc.* **1987**, *134*, 346; b) L. J. Krause, P. S. Lugg, T. A. Speckhard, *J. Electrochem. Soc.* **1989**, *136*, 1379; c) A. Viehbeck, M. J. Goldberg, C. A. Kovac, *J. Electrochem. Soc.* **1990**, *137*, 1460.
- [12] P. K. Bhowmik, A. H. Molla, H. Han, M. E. Gangoda, R. N. Bose, *Macromolecules* **1998**, *31*, 621.
- [13] a) C. A. Melendres, P. C. Lee, D. Meisel, *J. Electrochem. Soc.* **1983**, *130*, 1523; b) A. Kavanagh, K. J. Fraser, R. Byrne, D. Diamond, *ACS Appl. Mater. Interfaces* **2013**, *5*, 55.
- [14] R. J. Mortimer, J. L. Dillingham, *J. Electrochem. Soc.* **1997**, *144*, 1549.